Filtering Airborne Laser Scanner Data: A Wavelet-Based Clustering Method

T. Thuy Vu and Mitsuharu Tokunaga

Abstract

Filtering the airborne laser scanner data is challenging due to the complex distribution of objects on Earth's surface and it is still in development stage. This problem has been investigated so far with varieties of algorithms, but they suffer from different magnitudes of drawbacks. This study proposed a new and improved hybrid method based on multi-resolution analysis. Wavelet was adopted in this multi-resolution clustering approach. It enabled the classification of objects based on their size and the efficiency to filter out unwanted information at a specific resolution, and the proposed algorithm is named the ALSwave *(Airborne Laser Scanner Wavelet) method.* ALSwave *has been tested on two data sets acquired over the urban areas of Tokyo, Japan and Stuttgart, Germany. The results showed a well-filtered, bare earth surface coupled with acceptable computational time. The accuracy assessment was carried out by comparison between the filtered bare earth surface by* ALSwave *and the manually filtered surface. The Root Mean Square Error (RMSE) follows a linear relationship with respect to terrain slope. This wavelet-based approach has opened a new way to filter the raw laser data that subsequently generates fast and more accurate digital terrain models.*

Introduction

In the last decade there has been a proliferation of varied algorithms to filter the airborne laser scanner point clouds. The reason is that the airborne laser scanner has been considered and utilized as a highly accurate tool for topographic mapping. The major purpose of filtering can simply be described as a distinction between the bare earth points and the overlying object points. However, objects on the earth surface are complex, and affect the reflectance of a laser hit, consequently, a simple description cannot be accomplished easily (Vosselman and Maas, 2001). The existing algorithm could be categorized into two types, i.e., with or without interpolation of the point clouds into a regular grid. Filtering the grid-based laser point (Oude Elbrink and Maas, 2000; Acqua, *et al.*, 2001) is much faster and easier to implement but suffers from the problem of interpolation (Vosselman and Maas, 2001). This group employed the conventional image processing techniques such as texture analysis (Oude Elbrink and Maas, 2000) and low-pass or morphological filtering (Acqua, *et al.*, 2001). Alternatively, filtering of raw laser points could avoid the problems caused by interpolation, but requires intensive computation time; it has been implemented in recent studies (Kraus and Pfeifer, 1998; Maas and Vosselman, 1999; Axelsson, 2000). For example, in SCOPP++, the filter approach of Kraus and Pfeifer (1998) is implemented, and in TerraScan (Terrrasolid, Finland) the filter approach of Axelsson (2000) is implemented.

Generally, both groups of developed algorithms investigate the distribution of elevation points in a local area to determine whether a point is terrain or an off-terrain object point. However, how to choose the right size of this local area which is able to filter out completely overlying objects remains as a problem. For example, it is the size co-occurrence matrix in Oude Elbrink and Maas's (2000) approach or the size of filter kernel in Vosselman's (2000) approach. Most of these approaches face the same problem in removing the large overlying objects. A laser point reflecting from a large object shows no difference in elevation compared to its surroundings, and hence, it is classified as terrain point. In fact, the aforementioned problem is related to the size of the objects on the Earth's surface and could be classified by multi-resolution analysis.

Analysis of the objects in the image or the point clouds at different resolutions has been proved as an excellent approach to detect and extract the target objects (Lega, *et al.*, 1995; Starck and Murtagh, 1994). The key point is that the objects appear only within a certain range of scale, or resolution. The first application of multi-resolution processing airborne laser scanner data was introduced by Kraus and Pfeifer (2001) in terms of data pyramids; this algorithm was developed for vegetation-covered areas. In this study, the proposed algorithm concentrates on urban areas that consists of dense, man-made objects. To build up the multi-resolution space for filtering airborne laser scanner data, wavelet analysis is adopted. The idea of wavelet that originated in early 20th century has been an attractive tool with the solid mathematical background in the 1980's for several researchers and engineers of different fields. The proposed algorithm applies the redundant *a trous* algorithm with cubic spline wavelet functionality (Shensa, 1992) to maintain the translation invariant which is required for feature detection. In the next section, the *a trous* algorithm (Shensa, 1992) is presented followed by the proposed multi-resolution clustering method. It is followed by the information of the test area, employed airborne laser scanner data, and the test results.

The *A Trous* Wavelet Algorithm

The *a trous* algorithm (Shensa, 1992) is applied to build up a multi-resolution framework. Let $\Phi(x)$ and $\Psi(x)$ represent

T.T. Vu is with the Disaster Information System Team, Earthquake Disaster Mitigation Research Center (EDM), National Institute for Earth Science and Disaster Prevention (NIED), 1-5-2 Kaigandori, Wakinohama, Chuo-ku, Kobe 651-0073, Japan (thuyvu@edm.bosai.go.jp; thuygeo@yahoo.com).

M. Tokunaga is with Environmental System Engineering, Kanazawa Institute of Technology, 7-1, Ogigaoka, Nonoichi, Ishikawa 921-8501, Japan (mtoku@neptune.kanazawa-it.ac.jp).

Photogrammetric Engineering & Remote Sensing
Vol. 70, No. 11, November 2004, pp. 1267–1274.

0099-1112/04/7011–1267/$3.00/0

scaling and wavelet functions, respectively. The scaling function is chosen to satisfy the dilation equation as follows:

$$\frac{1}{2}\Phi\left(\frac{x}{2}\right) = \sum_{u} h(u)\Phi(x-u) \tag{1}$$

where h is a discrete low-pass filter associated with scaling function Φ, and u is its size.

This equation shows the link between two consecutive resolutions, which differs by a factor of 2, by the low-pass filtering. The wavelet function $\Psi(x)$ is defined by

$$\frac{1}{2}\Psi\left(\frac{x}{2}\right) = \Phi(x) - \frac{1}{2}\Phi\left(\frac{x}{2}\right). \tag{2}$$

In implementation, the smoothed discrete data $c_j(k)$ at a given resolution j and at position k can be obtained by the method of convolution:

$$c_j(k) = \sum_{u} h(u)c_{j-1}(k + 2^{j-1}u). \tag{3}$$

The difference between two consecutive resolutions is calculated as

$$w_j(k) = c_{j-1}(k) - c_j(k) \tag{4}$$

which presents the wavelet coefficients.

The cubic B-spline with the properties of compact support, symmetry, differentiability, and one zero-crossing was chosen to be a scaling function. The implementation for one-dimensional data is the convolution with the mask $\left[\frac{1}{16}\ \frac{4}{16}\ \frac{6}{16}\ \frac{4}{16}\ \frac{1}{16}\right]$, and the *a trous* algorithm is easily extended to the two-dimensional space. This leads to a convolution with a mask of 5×5 pixels for the wavelet connected to the cubic B-spline scaling function. The coefficients of the mask with all the elements scaled up to 256 are:

$$\begin{bmatrix} 1 & 4 & 6 & 4 & 1 \\ 4 & 16 & 24 & 16 & 4 \\ 6 & 24 & 36 & 24 & 6 \\ 4 & 16 & 24 & 16 & 4 \\ 1 & 4 & 6 & 4 & 1 \end{bmatrix}.$$

The above described wavelet algorithm is just a part of an entire wavelet clustering method proposed in this study which is developed for processing airborne laser scanner data. A cautious note should be made because the name of wavelet clustering is also utilized by other researches. The proposed method for filtering airborne laser data in this study is based on wavelet, and is called *ALSwave* (Airborne Laser Scanner Wavelet) method. The outline of this method is presented in the following section.

Wavelet Clustering Algorithm for Filtering Airborne Laser Scanner Data: The *ALSwave* Method

ALSwave is proposed as a semi-automatic algorithm to filter the airborne laser scanner data. The complete procedure of processing is shown in flowchart (Figure 1). The step-by-step details of this algorithm are described in the following subtopics.

Interpolation

There are myriads of the interpolation methods, and determination of the best and suitable interpolation method is beyond the scope of this paper. The planar interpolation method (Behan, 2000) on the triangulated irregular network (TIN) gives the most accurate interpolated image. Therefore, this method has been adopted in the *ALSwave* to serve as the first step of processing.

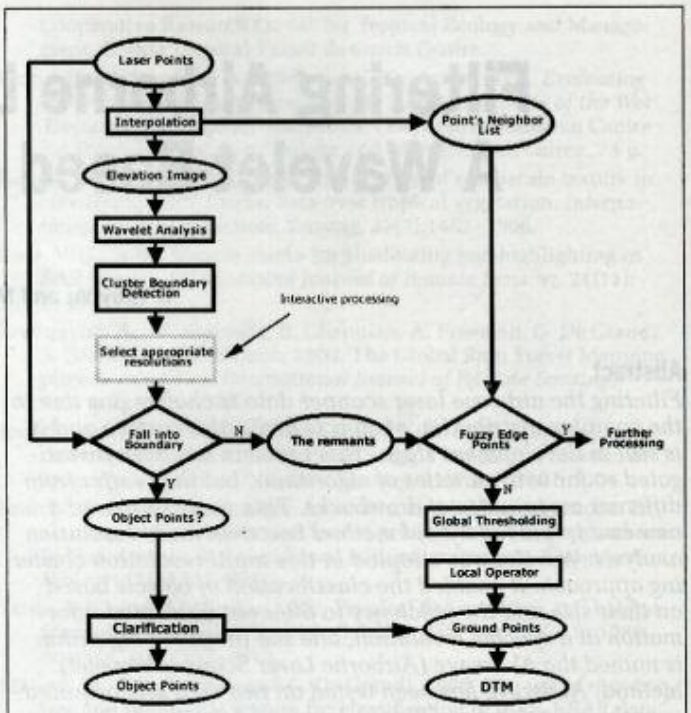

Figure 1. The flowchart of *ALSwave* processing.

Wavelet Analysis

Wavelet analysis is the core of the *ALSwave* method. The *a trous* algorithm as previously discussed is applied to build up the multi-resolution framework. It is noted that wavelet is one kind of the linear multi-resolution (or multi-scale) analysis which suffers from the distortion of the objects at a coarser resolution. To mitigate this problem, a median filter is applied prior to wavelet filtering. The wavelet analysis is outlined in terms of *pseudo* codes as follows:

- Input a parameter: the number of the resolutions to be analyzed, e.g., *kmax*.
- Init $k = 1$, i.e., scale equals 1
- Assign the original image to *im_in*
- For each k, k is increased by 1 until $k = kmax$
  - Median filter *im_in* with the kernel size equals to $2^k + 1$, obtain *im_med*
  - Detect the strong signatures by subtracting *im_in* and *im_med* and thresholding by a factor of 3σ, where σ is the standard deviation of the difference.
  - Assign *im_in* to *im_tmp*
  - Replace the values of the strong signatures in *im_tmp* by the ones in *im_med*
  - Wavelet filter *im_tmp*, obtain im_wave which is the wavelet-smoothed image at scale k.
  - The wavelet coefficients or detailed image is the difference between *im_wave* and *im_in*.
  - Assign *im_wave* to *im_in* for the next loop.

Wavelet analysis generates a family of smoothed and detailed images. These can be used to find the boundaries of the multi-resolution clusters which depict the existence of the objects based on their sizes. In wavelet analysis, the only input parameter is the number of resolutions which is decided by the operator. It should be noted that the more resolutions are employed, the more information we obtain, and hence more time is required to process the algorithm.

Cluster Boundary Detection

Across the multi-resolution space, the edge pixels are found as the cut points formed by the profiles of the consecutive

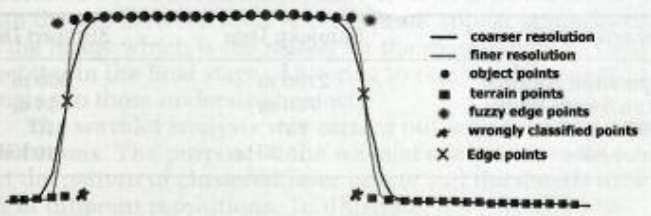

Figure 2. The illustration of the detecting edge pixels.

resolutions. A simple idea on how to detect the cluster boundaries is illustrated in Figure 2. However, due to the effect of interpolation and the gap between the laser points, the edges of the objects could not appear vertically. There is a buffer of edge pixels, named the *fuzzy edge* pixels. It should be noted that the real location of the edges of the objects must lie within the buffer zone.

Selection of the Appropriate Resolutions

An interactive processing approach is used where the operator must choose the appropriate resolutions for further processing. The decision is dictated by the distribution of the objects in the study area, and it operates on two limits. While the lower limit deals with the finer resolution that appears at an acceptable level of noise, the upper limit is related to the object's degree of distortion. Even though a median filter was applied to retain the strong signatures, the distortion still prevailed.

Detection of Object Points

By a simple spatial relation of *fall-into-boundary*, it is possible to distinguish between the qualified object points and the remnants. This processing step is a hybrid method in which the laser points are grouped and categorized based on the results obtained from the interpolated images. However, there is an ambiguity along the edges of the objects. Due to the unpredicted reflectance of laser hits on the objects and the effect of interpolation, several laser points might be classified to the wrong class. The following processing will clarify these points. Furthermore, the objects such as cars, trees, and poles, due to their small size, appeared as noise in the previous processing. Therefore, the laser points belonging to these objects still exist in the remnants.

Detection of the Fuzzy Edge Points and Clarification of the Wrongly Classified Points

The existence of fuzzy edge points has been discussed. These fuzzy edge points must appear within the remaining set acquired from the prior processing. It is necessary to filter them out from the bare earth points. It is obvious that the points belonging to the objects and located at the edges of the objects have a sharp leap in elevation when compared to the elevation of neighbors. Therefore, the elevation threshold is set to classify the fuzzy edge points from the bare earth points. This processing was performed locally using the Delaunay neighbors of the points.

Let OP is the object point set that has been detected and P as the remainder's set of points. The fuzzy edge point is a the set of point P_i, where P_i is a point in P but belongs to the Delaunay neighbors of a detected object point OP_k, and its elevation differs from the average elevation of that Delaunay neighbor set an amount less than a specific threshold. Equation 5 illustrates the mentioned description:

$$FEP = \left\{ \begin{array}{l} P_i : (P_i \backslash in\ P) \text{ and } (\mathrm{OP}_k \backslash in\ OP) \text{ and} \\ (P_i \backslash in\ N_k) \text{ and } \left| Z(P_i) - AveZ(N_k) \right| \le StdOP \end{array} \right\} \quad (5)$$

where FEP is the fuzzy edge point set, $StdOP$ is the given threshold, N_k is the Delaunay neighbor point set of object point OP_k, $Z(P_i)$ is the elevation of the point P_i, $AveZ(N_k)$ is the average of elevation in N_k, and $\backslash in$ denotes the "is-element-of" symbol.

However, prior to the detection of the fuzzy edge points, the wrongly classified laser points located along the edges of the objects should be clarified. The elevation threshold in the Delaunay neighbors could detect the ground laser points that had been classified as the object points. The wrongly classified point is the point OP_k, where OP_k is a point in OP but belongs to the Delaunay neighbors of a classified ground point P_i and its elevation differs from the average elevation of that Delaunay neighbor set at an amount less than a specific threshold (Equation 6):

$$WCP = \left\{ \begin{array}{l} OP_k : (OP_k \backslash in\ OP) \text{ and } (P_i \backslash in\ P) \text{ and} \\ (OP_k \backslash in\ N_i) \text{ and } \left| Z(OP_k) - AveZ(N_i) \right| \le StdP \end{array} \right\}. \quad (6)$$

where WCP is the wrongly classified point set, $StdP$ is the given threshold, N_i is the Delaunay neighbor point set of terrain point P_i, $Z(P_i)$ is the elevation of the point P_i, $AveZ(N_i)$ is the average of elevation in N_i, and $\backslash in$ denotes the "is-element-of" symbol.

Global and Local Thresholding

By the reflection from the complicated objects of the earth surface, there might appear some erroneous laser points with very high elevations on the ground. These points were easily removed by a statistical thresholding applied on cumulative histogram. Subsequently, a new Voronoi diagram is generated for the remaining set of points. There are a few object points remaining in this set of points and their elevations differs from their neighbors. A slope thresholding is carried out iteratively in the local Delaunay neighbor. Because a high-density airborne laser scanner data can produce more laser hits on the objects, the number of iterations is highly dependent on the density of airborne laser scanner. As a result, the bare earth points are detected which are ready for the reconstruction of the bare earth surface. Finally, based on the bare earth point set detected, a TIN of the bare earth surface is constructed. Subsequently, a grid-based bare earth surface is generated.

Test Area and the Acquired Airborne Laser Data

The typical urban areas in Shinjuku and Tokyo, Japan and Stuttgart, Germany were selected to test the competence of the proposed algorithm. The test areas were selected to cover two kinds of terrain; while the Shinjuku area is quite flat with a high density of man-made objects, the Stuttgart area consists of steeper slopes with less density of man-made objects. Furthermore, there are lots of buildings, along with crowded human activities in these areas. The narrow streets appear in the tiny spaces between the very complex structures of the buildings, and there exist numerous moving objects on the streets. Also, there are trees aligned along the streets and buildings. These objects with different sizes, interspersed with each other, typify the area. It is difficult to speculate the very complicated in filtering these laser points and reconstructing the bare earth surface. The selected areas have good potential to prove the capability of the multi-resolution approach; Figure 3 illustrates the digital surface model of the test areas represented as a TIN.

Table 1 shows the parameters of the acquired airborne laser scanner data over the test areas. Shinjuku data was provided by Kokusai Kogyo Co. Ltd, and Stuttgart data was provided through the testing program launched by ISPRS WG III/3, which was a subset of data acquired in European Organization for Experimental Photogrammetric Research (OEEPE) project for laser data acquisition.

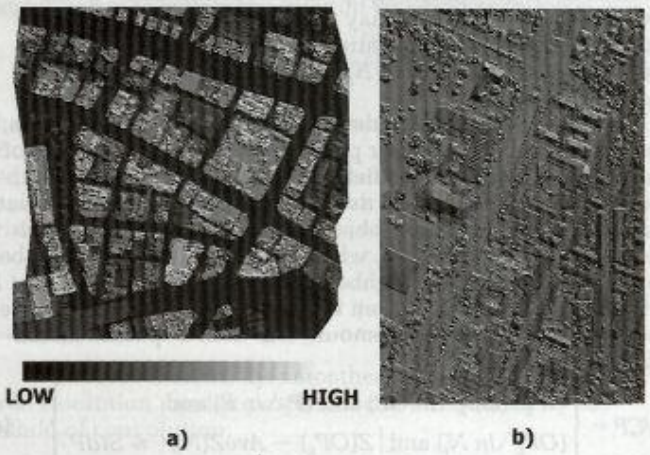

Figure 3. Digital Surface Model of the test areas represented in TIN: (a) Shinjuku area; (b) Stuttgart area.

The approximate laser point densities of acquired data are 0.2 points/m^2 and 0.81 points/m^2 for Shinjuku and Stuttgart, respectively. It was interesting to test the performance of the developed algorithm with different densities of laser data. Due to the big gaps between the laser points, it was impossible to detect the exact shape of some buildings, and hence it was difficult to distinguish the trees located near the buildings. The multi-resolution approach could classify the objects based on their sizes. Therefore, it is applicable in eliminating the unwanted trees located nearby the buildings. Both of the filtering methods, either directly on point clouds or indirectly on interpolated images faces unavoidable problem due to this low point density. It was for this reason that this study proposed a hybrid method approach for filtering laser scanner data.

TABLE 1. PARAMETERS OF AIRBORNE LASER SCANNER DATA

Parameters	Shinjuku Data	Stuttgart Data
Operation Altitude	2700 m	900 m
Scan Swath Width	720 m	144 m
FOV	16°	10°
Pulse Rate	15 KHz	10 KHz

Test Results

Airborne laser points were interpolated into 1 meter grid resolution. With the low point density, a denser-interpolated grid

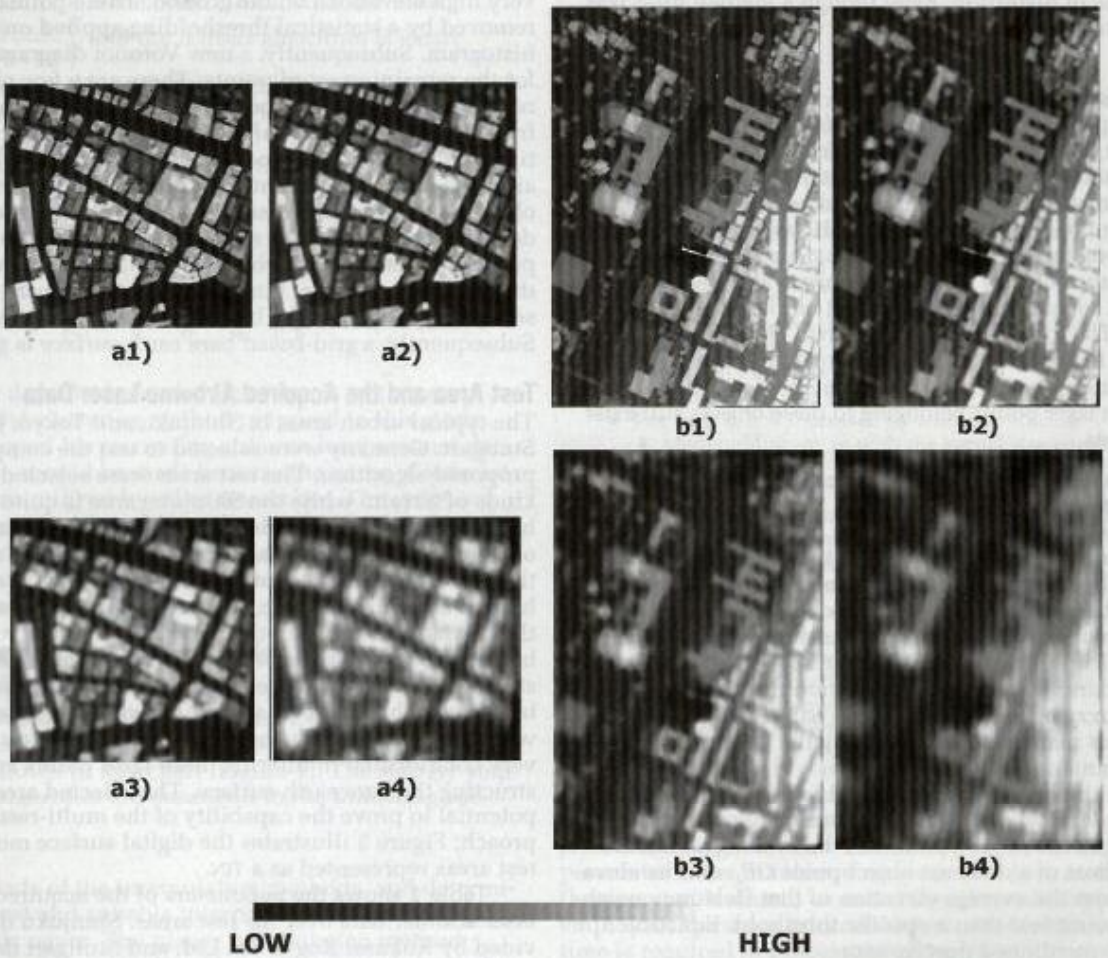

Figure 4. The wavelet-smoothed images across four consecutive resolutions: (a1), (a2), (a3) and (a4) Shinjuku area; (b1), (b2), (b3) and (b4) Stuttgart area.

resolution could not be achieved. The objects with a size less than the gap between laser points cannot appear appropriately in the image which is the reason for the requirement of local operator in the final stage of filtering to remove the points belonging to these undersized objects.

The wavelet analysis was carried out with four employed resolutions. The purpose of the wavelet analysis is to find out the pattern of clustered laser points and the details existing at different resolutions. To illustrate, the smoothed images at four consecutive resolutions are depicted in Figure 4. It is obvious to recognize the cluster distributions of the laser points which belong to the buildings in the test area. Moreover, these images clearly illustrate the idea of multi-resolution approach, i.e., the small objects disappear in the coarse resolutions. This is a great advantage to assist in the filtering task.

Consequently, the boundaries of clusters across different resolutions were distinguished as illustrated in Figure 5. Figure 5a1, Figure 5a2, Figure 5b1, and Figure 5b2 show the detected boundaries at the finer resolution which appears noisy. The coarser resolutions with the acceptable degrees of distortion, shown in Figure 5a3, Figure 5a4, Figure 5b3, and Figure 5b4 were selected as the appropriate resolutions to construct the boundaries of objects. Other filtering algorithms (Acqua, *et al.*, 2000; Vosselman, 2000) employed mathematical morphology. While the former was processed in a grid-based format, the latter was processed directly in the raw laser points. Both of them had considered the kernel size prior to the application of filtering in a certain area, which often failed to yield good output. Practically, it is difficult to obtain the right kernel size. The wavelet-based algorithm proposed in this study avoids that difficulty by analyzing the data in a multi-resolution space. Simultaneously, the boundaries of clusters are detected and the multi-resolution domain is formed to allow the selection of the appropriate resolutions.

The interpolation of the laser points into grid causes the mixture of the bare earth points and the overlying object points (Vosselman and Mass, 2001). However, to take the advantage of easy implementation and highly efficient computational time, the proposed algorithm detected the boundaries of the clusters in a grid-based format. To distinguish the laser points belonging to the objects, a spatial relation of fall-into-boundary was applied. The effect of interpolation could be adjusted at this step by the combined analysis, both in the detected boundaries and on the raw laser points. The threshold value of 3 meters allowed for the reclassification of the laser points along the edges of the objects which belong to the bare earth surface, but were originally classified as the overlying object points in the previous processing. Subsequently, the fuzzy edge points were also identified with the threshold value of 7 meters, as observed in the test area. Prior to the application of the local operator to remove the laser points belonging to the small objects, a threshold value of 90 percent was applied in cumulative histogram with Shinjuku data. This step discarded some laser points with very high elevations and dissimilar from the remnants. It was impossible to

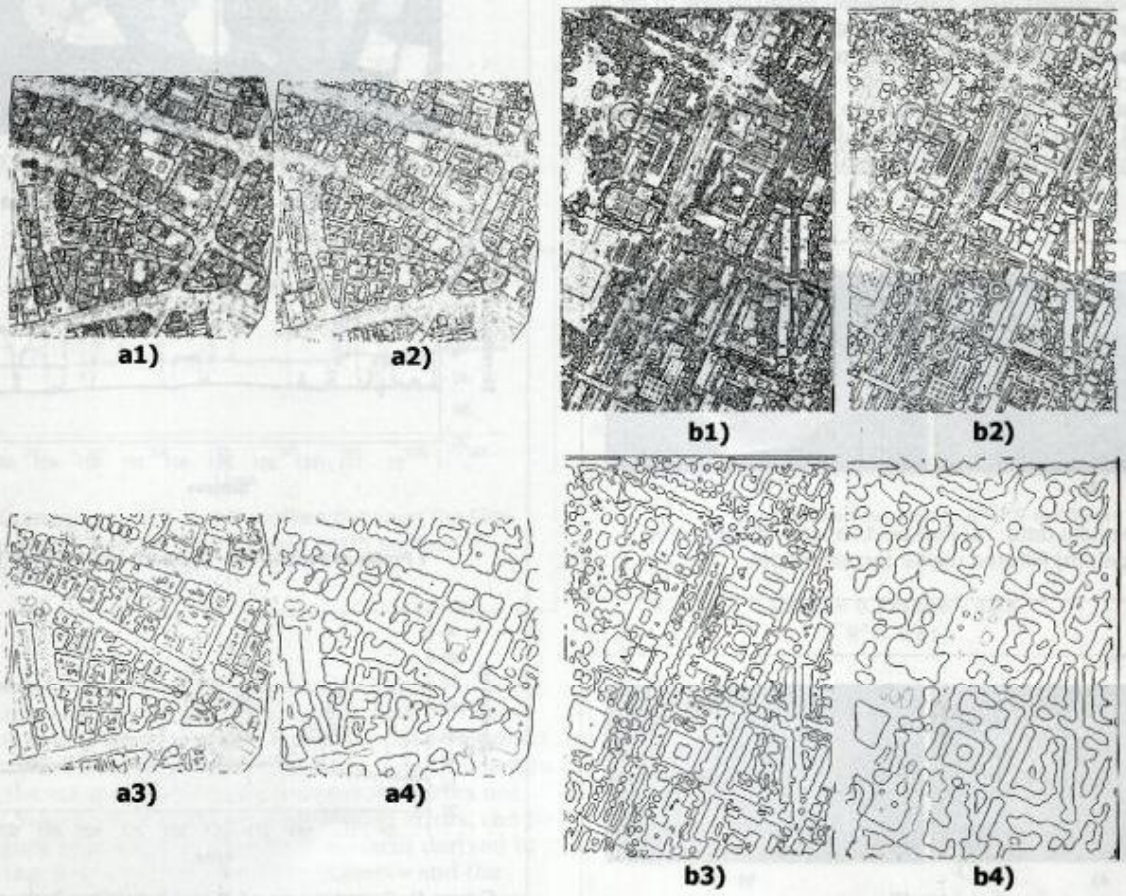

Figure 5. The detected boundaries of clusters across four consecutive resolutions: (a1), (a2), (a3) and (a4) Shinjuku area; (b1), (b2), (b3) and (b4) Stuttgart area.

apply global thresholding for Stuttgart data where the terrain is steeper, i.e., no steep section on its cumulative histogram.

The final stage of filtering was based on the local operator. After global thresholding, a new Voronoi diagram was generated for the remaining set of points. In processing the test area, the angle of 10 degrees was given as a slope threshold. This processing step is similar as the method developed by Axelsson (2000). However, the iterative slope thersholding here was carried out more easily while the large objects had been already removed. The local threshold was applied iteratively three times for Shinjuku data, and six times for Stuttgart data because of higher densities of laser points. As a result, the detected bare earth points were used to reconstruct the bare earth surface of the test area. Figure 6 and Figure 7 show both the bare earth surfaces and the original digital surface models to visually compare the results of filtering for Shinjuku area and Stuttgart area, respectively.

Figure 6b and Figure 7b show the bare earth surfaces with no significant presence of noise by overlying objects. Because the detection was based on the size of the objects, *ALSwave* could avoid the problem of removing the large buildings, which were not solved by mathematical morphology (Vosselman and Maas, 2001). However, the test area consisted no objects like dikes or lakes the laser points belonging to this type of object could not be classified as the bare earth points by *ALSwave*. These points could be recovered with the help of an additional data source which can provide an additional property of object, such as spectral information. Table 2 summarizes the point classes and their quantities. It is obvious that there is a small amount of laser points belonging to the bare earth surface, i.e., 8.03 percent or 13.29 percent which typifies a dense, urban area. This filtered result needs to be verified either with ground survey data or with a large-scale topographic map, unfortunately, were not available when this study was carried out.

Figure 8 and Figure 9 illustrate the X, Y profiles comparing the digital surface models and the detected bare earth surfaces. They show very effective results of filtering. The

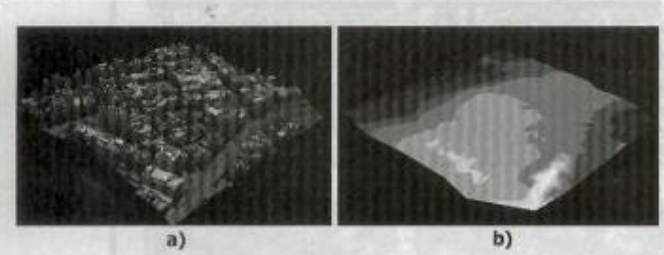

Figure 6. Shinjuku data: (a) Perspective view of the digital surface model; (b) Filtered digital terrain model.

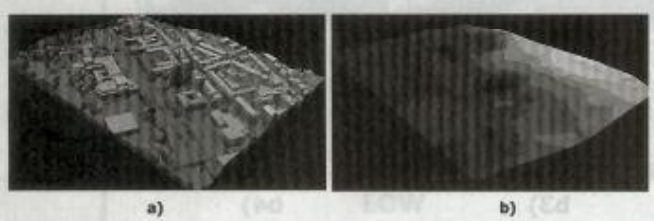

Figure 7. Stuttgart data: (a) Perspective view of the digital surface model; (b) Filtered digital terrain model.

TABLE 2. RESULTS OF *ALSWAVE* FILTERING IN THE TEST AREA

Class	Number of Points		Percentage (%)	
	Shinjuku	Stuttgart	Shinjuku	Stuttgart
Bare earth points	5272	32359	8.03	13.29
Overlying objects (building)	36565	145684	55.71	59.85
Fuzzy edge points	8639	19731	13.16	8.10
Wrongly classified points	1913	1813	2.91	0.75
Dissimilar very high elevation points	2505	0	3.82	0
Small objects (Detected by local operator)	10742	43812	16.37	18.01

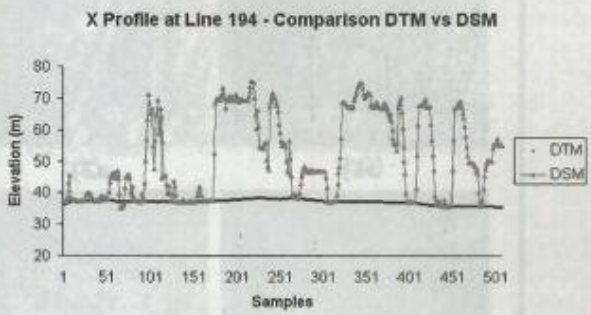

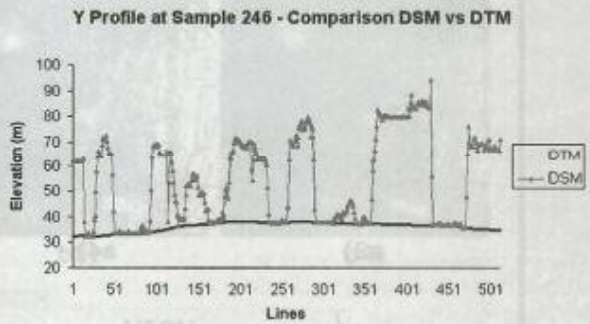

Figure 8. Comparison of X and Y profiles between the Digital Surface Model and the filtered bare earth surface of Shinjuku area.

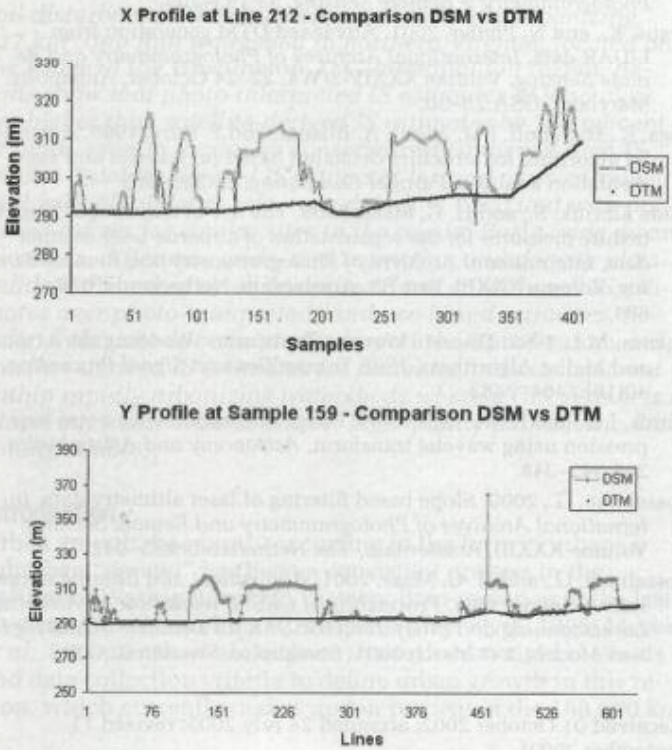

Figure 9. Comparison of X and Y profiles between the Digital Surface Model and the filtered bare earth surface of Stuttgart area.

original set of laser points was also manually filtered in order to obtain an accurate reference of the filtered, bare earth surface. This manually filtered surface is used for the assessment of the accuracy in filtering by *ALSwave*. It is a good procedure for checking the accuracy of filtering because the errors not caused by *ALSwave*, such as the scanner system errors, can be excluded. Figure 10 shows the bare earth surfaces derived by manual filtering. It is noted that in both *ALSwave* and the manual method, the elevated way in the study area was considered as a bare earth surface because of its gradual change in elevation. Visually, both filtered results yielded the quite similar bare earth surfaces, even though the result derived by

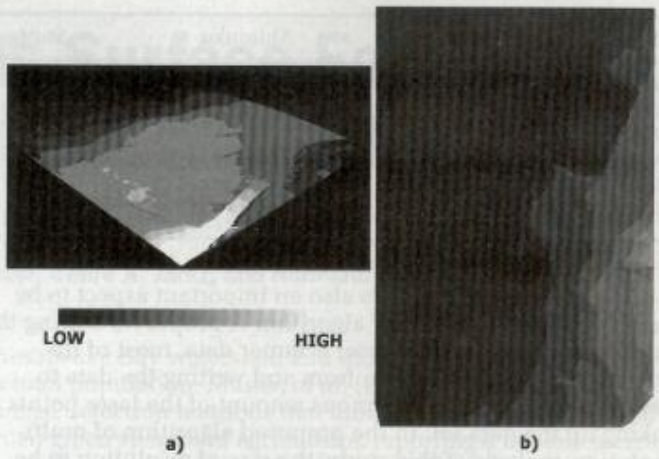

Figure 10. The bare earth surface by manual filter: (a) Shinjuku area; (b) Stuttgart area.

ALSwave could not retain well the break lines, such as bridges and elevated ways, as the one derived by manual method. The problem of retaining break lines from *ALSwave* can be observed in the middle of the X profile in Figure 9 where the subway opening is crossed. Quantitatively, two filtered results were compared point-by-point in the whole area to obtain the statistical comparison. The quantitative comparison was also conducted in different parts of the test area consisting of different terrain slopes. The results are shown in Table 3, and based on this accuracy assessment, the relationship between RMSE and terrain slope was discovered as illustrated in Figure 11. The RMSE gets worse than 1 meter if the slope terrain is steeper than 3.6 degrees.

TABLE 3. QUANTITATIVE ASSESSMENT OF ACCURACY

	Mean (meter)		STD (meter)		RMSE (meter)		Slope (radian)	
	A	B	A	B	A	B	A	B
Whole area	0.204	0.605	0.424	1.155	0.470	1.303	0.037	0.065
Flat area	0.107	0.127	0.116	0.339	0.158	0.362	0.025	0.025
Steeper area	0.294	0.564	0.442	0.930	0.531	1.087	0.056	0.064

(STD: Standard Deviation; RMSE: Root Mean Square Error; A: Shinjuku area; B: Stuttgart area).

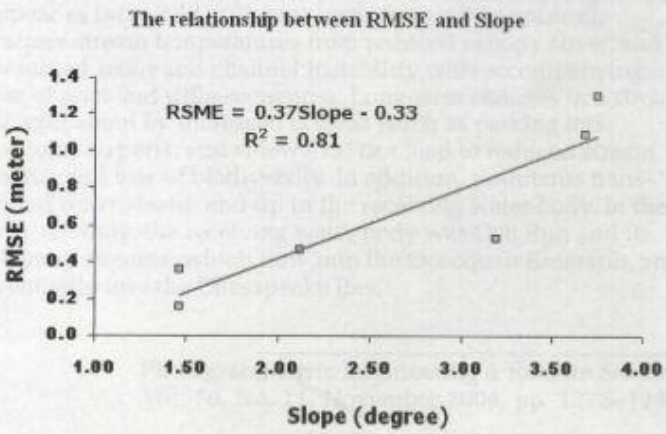

Figure 11. Relationship of RMSE and terrain slope.

TABLE 4. COMPUTATION TIME ACROSS 4 RESOLUTIONS EMPLOYED

Processing Step (second)	Shinjuku	Stuttgart
Interpolation	4	15
Wavelet analysis	21	24
Detect boundaries	114	113
Raster-to-vector	3	4
Global and local threshold	15	117
Total	157	273

The computation time is also an important aspect to be considered whenever a new algorithm is proposed. During the processing of the airborne laser scanner data, most of the time is used reading the data from and writing the data to files. This is due to the enormous amount of the laser points making up the data set. In the proposed algorithm of multi-resolution analysis of this study, the size of resolution to be employed is the main factor that controls the computation time. If the time required for input and output of the data and the time needed for interactive processing is excluded, the total computation time for the processing will be substantially lower. For instance, the computation time for the test areas carried out on a PC with a 600MHz CPU and memory of 128MB is illustrated in Table 4. Until now, there have been no reports regarding the computation time for the existing algorithms; therefore, comparing the attained time efficiency with other algorithms is not possible.

Conclusions

A new approach named *ALSwave* with wavelet analysis has been introduced to process airborne laser scanner data. *ALSwave* analyzes the laser points in a multi-resolution space, and hence, is able to mitigate the difficulties involved in filtering them. Furthermore, a hybrid analysis approach, in both grid-based and raw laser points, has been proposed in *ALSwave* to take the advantages of easy implementation and highly efficient computation time of grid-based processing and adjust the effect of interpolation with the raw laser points. *ALSwave* was tested in two dense urban areas in Tokyo, Japan, and Stuttgart, Germany with two different densities of airborne laser scanner data. It yielded very good results for filtering when compared to the manually filtered DTM. This study also discovered a linear relationship between RMSE in filtering by *ALSwave* and the terrain slope which is very useful finding for any application or further improvement of *ALSwave*. The verification and the testing of the proposed algorithm in a variety of terrain types will be carried out in future studies utilizing the detected boundaries of the point clusters in reconstruction the overlying objects in an urban area.

Acknowledgments

The data adopted in this research were provided by Kokusai Kogyo Co. Ltd, Japan and the testing program of ISPRS Commission III/3, which provided the data set acquired by FOTONA AS, Norway in OEEPE project on laser scanner data acquisition.

References

Acqua, F.D., P. Gamba, and A. Mainardi, 2001. Digital Terrain Models in dense urban areas, *International Archives of Photogrammetry and Remote Sensing*, Volume XXXIV-3/W4, 22–24 October, Annapolis, Maryland, USA:195–202.

Axelsson, P., 2000. DEM generation from laser scanner data using adaptive TIN models, *International Archives of Photogrammetry and Remote Sensing*, Volume XXXIII, Part B4, Amsterdam, Netherlands:111–118.

Behan, A., 2000. On the matching accuracy rasterised scanning laser altimeter data, *International Archives of Photogrammetry and Remote Sensing*, Volume XXXIII, Amsterdam, The Netherlands: 75–82.

Kraus, K., and N. Pfeifer, 1998. Determination of terrain models in wooded areas with airborne laser scanner data, *ISPRS Journal of Photogrammetry & Remote Sensing*, 53:193–203.

Kraus, K., and N. Pfeifer, 2001. Advanced DTM generation from LIDAR data, *International Archives of Photogrammetry and Remote Sensing*, Volume XXXIV-3/W4, 22–24 October, Annapolis, Maryland, USA:23–30.

Lega, E., H. Scholl, J.M. Alimi, A. Bijaoui, and P. Bury, 1995. A parallel algorithm for structure detection based on wavelet and segmentation analysis, *Parallel Computing*, 21:265–285.

Oude Elbrink, S., and H.-G. Maas, 2000. The use of anisotropic height texture measures for the segmentation of airborne laser scanner data, *International Archives of Photogrammetry and Remote Sensing*, Volume XXXIII, Part B3, Amsterdam, Netherlands: 678–684.

Shensa, M.J., 1992. Discrete Wavelet Transforms: Wedding the à trous and Mallat Algorithms, *IEEE Transactions on Signal Processing*, 40(10):2464–2482.

Starck, J.L., and F. Murtagh, 1994. Image restoration with noise suppression using wavelet transform, *Astronomy and Astrophysics*, 288:342–348.

Vosselman, G., 2000. Slope based filtering of laser altimetry data, *International Archives of Photogrammetry and Remote Sensing*, Volume XXXIII, Amsterdam, The Netherlands:935–942.

Vosselman, G., and H.-G. Maas, 2001. Adjustment and filtering of raw laser altimetry data, *Proceeding of OEEPE workshop on Airborne Laserscanning and Interferometric SAR for Detailed Digital Elevation Models*, 1–3 March 2001, Stockholm, Sweden:62–72.

(Received 01 October 2002; accepted 24 July 2003; revised 11 September 2003)